Liquid Crystals

Publication details, including instructions for authors and subscription information:
http://www.informaworld.com/smpp/title~content=t713926090

New series of chiral ferroelectric liquid crystals with the keto group attached to the molecule core

V. Hamplová[a]; A. Bubnov[a]; M. Kasˇpar[a]; V. Novotná[a]; M. Glogarová[a]
[a] Institute of Physics, Academy of Sciences and the Czech Republic, Na Slovance 2, 18221 Prague 8, Czech Republic,

To cite this Article Hamplová, V. , Bubnov, A. , Kasˇpar, M. , Novotná, V. and Glogarová, M.(2003) 'New series of chiral ferroelectric liquid crystals with the keto group attached to the molecule core', Liquid Crystals, 30: 4, 493 — 497

To link to this Article: DOI: 10.1080/0267829031000090869

URL: http://dx.doi.org/10.1080/0267829031000090869

LIQUID CRYSTALS, 2003, VOL. 30, NO. 4, 493–497

Taylor & Francis
Taylor & Francis Group

New series of chiral ferroelectric liquid crystals with the keto group attached to the molecule core

V. HAMPLOVÁ, A. BUBNOV*, M. KAŠPAR, V. NOVOTNÁ and
M. GLOGAROVÁ

Institute of Physics, Academy of Sciences and the Czech Republic, Na Slovance 2,
18221 Prague 8, Czech Republic

(*Received 9 September 2002; accepted 19 November 2002*)

Two new series of ferroelectric liquid crystals with a keto group attached to the molecular core and a lactate unit as a chiral centre were synthesized and studied. All the compounds exhibit the paraelectric SmA phase and the ferroelectric SmC* phase over very wide temperature ranges and down to room temperature. The main characteristics of the chiral ferroelectric SmC* phase, namely spontaneous polarization, spontaneous tilt angle, and dielectric constant, have been measured to establish their relationship to the length of the terminal chains. The influence of the chiral and non-chiral chain lengths on the helix pitch length is also discussed.

1. Introduction

In most ferroelectric liquid crystalline (FLC) materials the terminal chains are attached to the mesogenic core of the molecule by two groups with different electron affinities, for example, an ether group for the non-chiral chain and an ester group for the chiral chain, giving a strong longitudinal dipole moment.

In designing new chiral liquid crytalline materials, we have tried to weaken the longitudinal molecular dipole moment; this could result in a relative enhancement of the transversal dipole moment near the chiral centre, and thus lead to a stabilization of not only the ferroelectric phase but also the antiferroelectric phase. Keto and ester groups at opposite ends of the biphenyl unit almost compensate the longitudinal dipole moment of this part of the mesogen, and only a small contribution caused by the polar groups on the last phenyl ring remains non-compensated. Recently, it has been found by Kumar and Pisipati that for compounds with molecules in which the longitudinal dipole moment has been suppressed in a similar way, the antiferroelectric phase occurs [1]. Using the keto group instead of the ether group to connect one chain with the molecular core, in some cases can also lead to a substantial increase in the value of the spontaneous polarization, as was described by Yoschizawa *et al.* [2].

Two new series of liquid crystals with a keto group and two ester groups attached to the molecular core have been synthesized and studied. The general chemical formulae of the studied FLC materials are given below

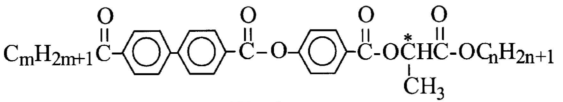

$C_mH_{2m+1}CO{-}C_6H_4{-}C_6H_4{-}COO{-}C_6H_4{-}COO\overset{*}{C}H(CH_3)COOC_nH_{2n+1}$

K m/n

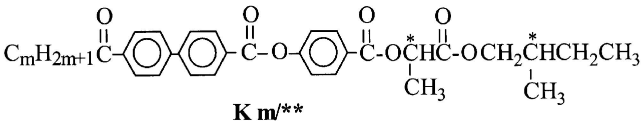

$C_mH_{2m+1}CO{-}C_6H_4{-}C_6H_4{-}COO{-}C_6H_4{-}COO\overset{*}{C}H(CH_3)COOCH_2\overset{*}{C}H(CH_3)CH_2CH_3$

K m/**

The compounds are referred to as **K*m*/*n*** and **K*m*/**** with one and two chiral centres, respectively, where ***m*** and ***n*** are the numbers of carbon atoms in the hydrocarbon chains of the molecule. The **K*m*/**** compound have a second branched chain, the (*S*)-2-methylbutoxy group.

2. Synthesis

The general procedure for the preparation of the **K*m*/*n*** and **K*m*/**** homologues is summarized in the scheme. The structures of the intermediates and final products were characterized by ^{1}H NMR spectroscopy using a 200 MHz Varian NMR spectrometer of solutions in $CDCl_3$, with tetramethylsilane as an internal standard.

2.1. *Acylbiphenyls 1*

A solution of the appropriate acylchloride (0.5 mol) in 1,2-dichloroethane was added dropwise into a mixture of 77 g of biphenyl and 78 g of anhydrous aluminium

---

*Author for correspondence; e-mail: bubnov@fzu.cz

Liquid Crystals ISSN 0267-8292 print/ISSN 1366-5855 online © 2003 Taylor & Francis Ltd
http://www.tandf.co.uk/journals
DOI: 10.1080/0267829031000090869

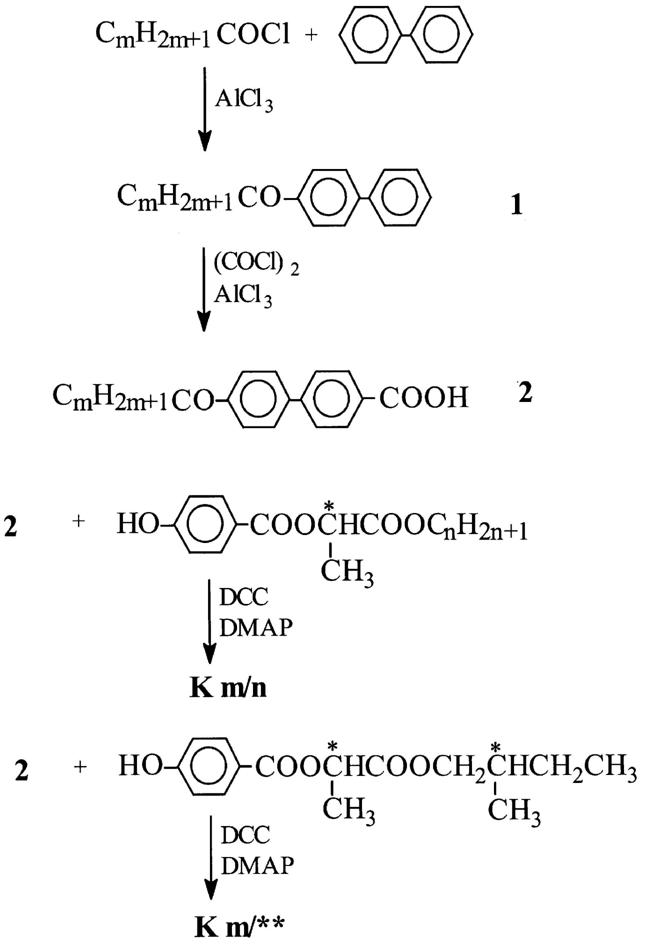

Scheme. Synthesis of **K*m*/*n*** and **K*m*/**** series.

chloride in 300 ml of dichloroethane. The reaction mixture was stirred at room temperature for four days; then, the mixture was poured into 500 g of ice with 200 ml of concentrated HCl. The organic layer was washed with water and let to stand overnight in the refrigerator. The yellow product was collected and recrystallised from dioxane; yield 70–75%. ^{1}H NMR (200 MHz, $CDCl_3$) for ***m*** = 6: 8.05 d (2H, *ortho* to *R*CO–); 7.65 and 7.70 dd (4H, *ortho* to –Ar); 7.4–7.5 m (3H Ar); 3.0 t (2H, CH_2CO); 1.2–1.7 m (8H, CH_2); 0.89 t (3H, CH_3).

2.2. *4′-Acylbiphenyl-4-carboxylic acids 2*

Oxalylchloride (25.2 g, 0.2 mol) was added to a stirred suspension of anhydrous aluminium chloride (26.6 g, 0.2 mol) in 200 ml of dry 1,2-dichloroethane at −10°C. A solution of 0.1 mol alkylxenylketone **1** in 50 ml of dry 1,2-dichloroethane was added dropwise to the stirred acylation mixture during one hour, keeping its temperature below 15°C during the reaction. The reaction mixture was stirred for 3 h at room temperature and left to stand overnight. It was then slowly poured into a stirred mixture of ice (200 g) and concentrated HCl (50 ml). The mixture was stirred for 2 h and the organic layer separated off, washed with water and evaporated to dryness. The solid was washed with petroleum ether or heptane and crystallized from dioxane/ethanol 1/1 mixture. The residual ketone was removed by extraction with *n*-heptane. The keto acids were purified by the extraction of sparingly soluble potassium salts with an excess of ethyl alcohol and a small amount of water, followed by acidification with diluted HCl. The white solids were dried in vacuum; yield 40–50%. ^{1}H NMR (200 MHz, $CDCl_3$) for ***m*** = 6: 8.19 d (2H, *ortho* to COOH); 8.07 d (2H, *ortho* to *R*CO–); 7.72 m (4H *ortho* to –Ar); 3.0 t (2H, CH_2CO); 1.2–1.6 m (8H, CH_2); 0.9 t (3H, CH_3).

2.3. ***Km*/*n*** *and* ***Km*/****

The **K*m*/*n*** and **K*m*/**** compounds were obtained by the usual esterification method using (*S*)-alkylactate or (*S*),(*S*)-methylbutyllactate units as chiral groups [3]. All crude products were carefully purified by column chromatography on silica gel (Kieselgel 60, Merck, Darmstadt) using a mixture of dichloromethane and ethanol (99/1) as eluent. After crystallization from ethanol the product purity was determined by high pressure liquid chromatography using an Ecom HPLC chromatograph and a Separon 7 μm, 3 × 150, Tessek silical gel column with a mixture of 99.9% toluene and 0.1% methanol as eluent. The eluting products were detected by a UV-Vis detector ($\lambda = 290$ nm). ^{1}H NMR (200 MHz, $CDCl_3$) for **K6/****: 8.29 d (2H, *ortho* to COOAr); 8.18 d (2H, *ortho* to –COOC*); 8.07 d (2H, *ortho* to RCO–); 7.76 m (4H, *ortho* to –Ar); 7.34 d (2H, *ortho* to –OCOAr); 5.35 q (1H, ArCOO$\underline{C}$H*), 4.02 m (2H, *CCOOC$\underline{H}_2$), 3.0 t (2H, CH_2CO); 1.64 d (3H, CH_3 lactate), 1.2–1.8 m (11H, CH_2, CH); 0.90 m (9H, CH_3).

3. Experimental results

3.1. *Sample preparation*

The samples were filled into glass cells with ITO transparent electrodes and polyimide layers unidirectionally rubbed, ensuring a planar (bookshelf) geometry. The sample thickness was defined by mylar sheets as 25 μm. The alignment was improved by using an electric field (40 kV cm^{-1}) of frequency 10–20 Hz, applied for 5–25 min depending on the material.

3.2. *Mesomorphic properties*

For all the substances, the phase behaviour and phase transition temperatures were determined on cooling from the isotropic phase on the basis of characteristic textures and their changes observed in planar cells using the polarizing microscope (Nikon Eclipse E600POL). The mesomorphic properties of all the new **K*m*/**** and **K*m*/*n*** compounds are collected in table 1. The phase diagrams for the **K*m*/**** and **K8/*n*** homologous series are shown in figures 1 and 2, respectively.

All the **K*m*/*n*** and **K*m*/**** compounds studied exhibit SmA and SmC* phases each over broad temperature ranges. The ferroelectric SmC* phase is partially monotropic for all the compounds studied (see table 1).

It can be seen from the phase diagrams that the width of the SmA phase as well as that of the ferroelectric SmC* phase, remains essentially constant on changing the non-chiral chain length (***m***) for both the **K*m*/*n*** and **K*m*/**** series. The length of the chiral chain (***n***) has a more pronounced influence on the mesomorphic properties (see figure 2): the width of the SmA phase increases on increasing the chiral chain length, while the width of the SmC* phase slightly decreases. Moreover, the temperatures of the phase transitions (SmA–SmC* and SmC–Crystal) shift slightly to lower temperatures on increasing the chiral chain length.

Table 1. Transition temperatures (°C) measured on cooling (5 K min^{-1}) and melting points (°C) for the homologous series **K*m*/**** and **K*m*/*n***. Cr = the crystal phase; SmC* = the ferroelectric smectic C phase; SmA = the paraelectric chiral smectic A phase; I = isotropic phase.

Compound	m.p.	Cr		SmC*		SmA		I
K6/**	90	•	44	•	129	•	160	•
K7/**	82	•	45	•	132	•	153	•
K8/**	83	•	38	•	132	•	153	•
K9/**	63	•	52	•	133	•	154	•
K6/4	98	•	28	•	126	•	169	•
K6/5	79	•	34	•	113	•	165	•
K6/6	76	•	30	•	104	•	162	•
K7/4	93	•	42	•	131	•	165	•
K8/4	84	•	45	•	134	•	165	•
K8/5	86	•	42	•	118	•	159	•
K8/6	85	•	42	•	120	•	160	•
K8/8	82	•	28	•	102	•	154	•
K8/9	90	•	30	•	94	•	155	•
K9/6	86	•	65	•	121	•	155	•
K9/9	85	•	55	•	104	•	148	•

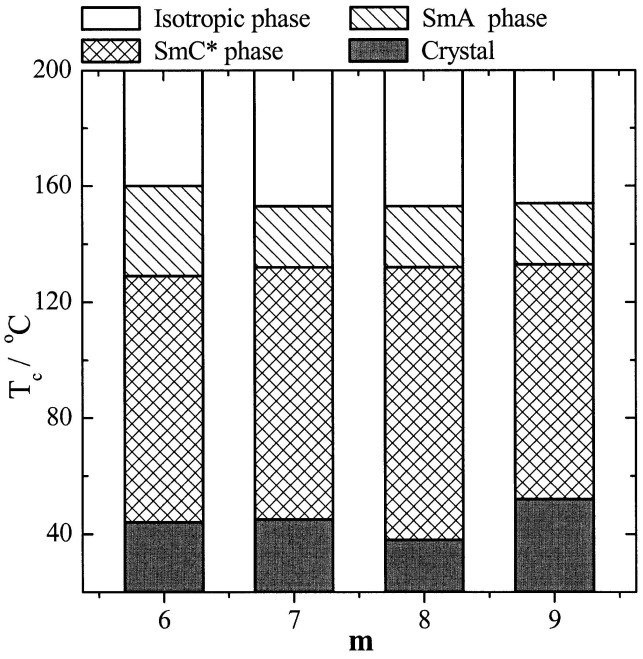

Figure 1. Phase diagram for the **K*m*/**** series measured on cooling.

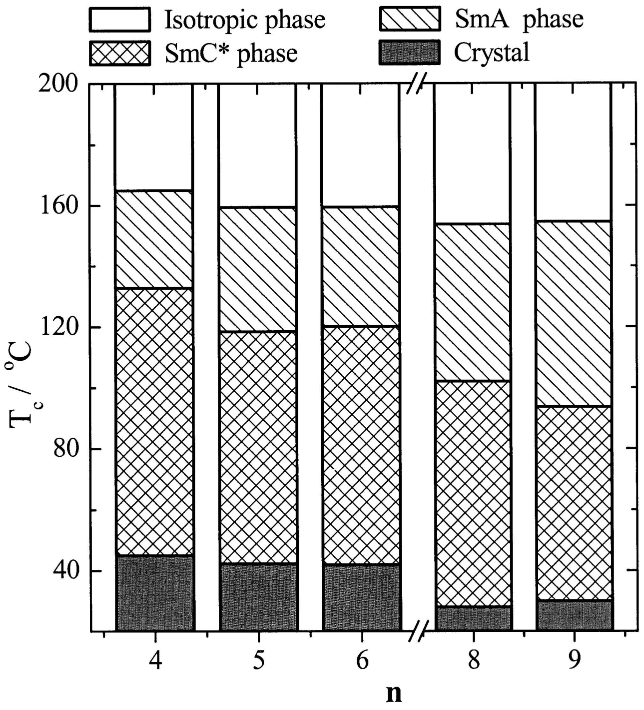

Figure 2. Phase diagram for the **K8/*n*** series measured on cooling.

3.3. *Spontaneous polarization and spontaneous tilt angle*

The values of the spontaneous polarization ($\mathbf{P}_s$) were evaluated from the $\mathbf{P}(\mathbf{E})$ hysteresis loop detected during $\mathbf{P}_s$ switching in an a.c. electric field $\mathbf{E}$ of frequency 60 Hz. The values of the spontaneous tilt angle (θ_s) were determined optically from the difference between extinction positions at crossed polarizers under opposite d.c. electric fields $\pm 40\,\mathrm{kV\,cm^{-1}}$.

The temperature dependence of the spontaneous polarization for the **K8/*n*** series is shown in figure 3. For the homologues with the shortest chains, no saturation in the $\mathbf{P}_s$ values was observed on cooling. For all the materials studied, both the spontaneous polarization and the tilt angle increase continuously from zero as the temperature decreases from the SmA–SmC* phase transition temperature (see figures 3 and 4, respectively). This behaviour is a typical manifestation of a second order phase transition. The **K*m*/**** compounds having two chiral centres have significantly higher values of $\mathbf{P}_s$ than the **K*m*/*n*** homologues, reaching values of about 200 nC cm^{-2} with no saturation at low temperatures. In addition, decreasing values of the spontaneous polarization, and also of the spontaneous tilt angle, with increasing ***n*** can be clearly seen in figure 3, figure 4 and table 2.

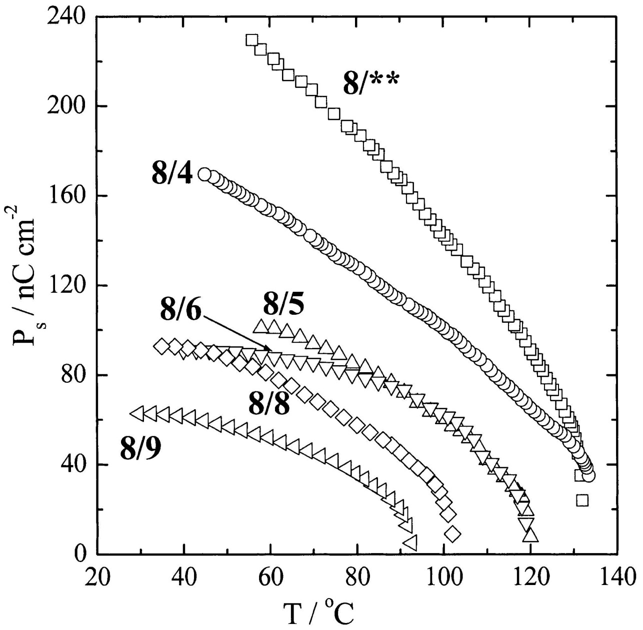

Figure 3. Temperature dependence of the spontaneous polarization for the **K8/*n*** series.

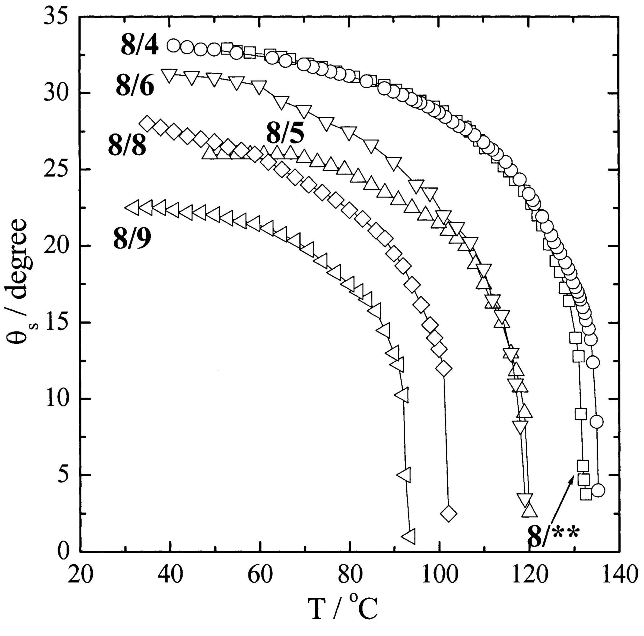

Figure 4. Temperature dependence of the spontaneous tilt angle for **K8/*n*** compounds.

Table 2. Values of spontaneous polarization (nC cm^{-2}), spontaneous tilt angle (°) and helix pitch length (μm) measured in the ferroelectric SmC* phase at the temperature $T_c - 50$ K.

m	*n*	$\mathbf{P}_s$	θ_s	*p*
6	**	191	31	0.8
7	**	195	33	1.1
8	**	201	32	1.2
9	**	195	34	1.3
6	**4**	147	29	0.9
6	**5**	136	29	1.1
6	**6**	115	23	1.5
7	**4**	154	32	1.3
8	**4**	136	32	1.4
8	**5**	101	26	2.1
8	**6**	89	30	3.2
8	**8**	90	27	4.8
8	**9**	62	23	3.8
9	**6**	88	32	—
9	**9**	44	28	—

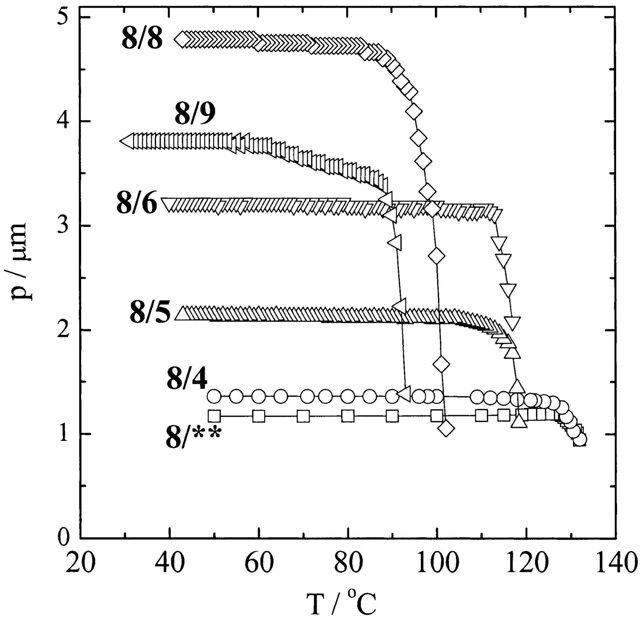

Figure 5. Temperature dependence of the helix pitch length for **K8/*n*** compounds.

3.4. *Helix pitch length*

The temperature dependence of the helix pitch length (*p*) (see figure 5 for **K8/*n*** compounds and table 2 for the values of *p* at T_c–50 K for all compounds studied) have been established by the diffraction of He-Ne laser light (630 nm) on disclination lines. The line spacing equals *p*. The values of *p* could not be measured over the whole temperature range of the SmC* phase for some materials, because at low temperatures the helix spontaneously unwinds. It could not be measured at any temperature for **K9/6** and **K9/9** because the dechiralization line spacing was rather large and irregular, which means that the helix remains almost unwound within the SmC* phase temperature range.

The helix pitch length was found to be almost temperature-independent over the whole temperature range of the SmC* phase with the exception of a region of a few degrees near the phase transition temperature from the SmA phase. For all compounds, *p* increases on increasing the number of carbon atoms in the chiral chain up to ***n*** = 8 (see figure 5 for **K8/*n*** compound and table 2). In addition, the helix pitch also increases with the number of carbon atoms in the non-chiral chain (see table 2).

3.5. *Dielectric constant*

The temperature dependence of the complex permittivity has been measured on cooling for all the compounds studied using a Schlumberger 1260 impedance analyser at frequencies of 30 and 100 Hz. In addition, the frequency dispersion of the real and imaginary parts of the permittivity has been measured in the frequency range from 1 Hz to 1 MHz in the SmC* and SmA phases.

The temperature dependence of the complex permittivity measured at a frequency of 100 Hz is shown in figure 6. There is a considerable increase in the permittivity on cooling from the SmA phase to the SmC* phase due to the strong contribution of the Goldstone mode. The frequency dispersion data showed the Goldstone mode in the ferroelectric SmC* phase and the soft mode in the paraelectric SmA phase. The detailed dielectric frequency dispersion data and a discussion of the dielectric properties will be published elsewhere [4].

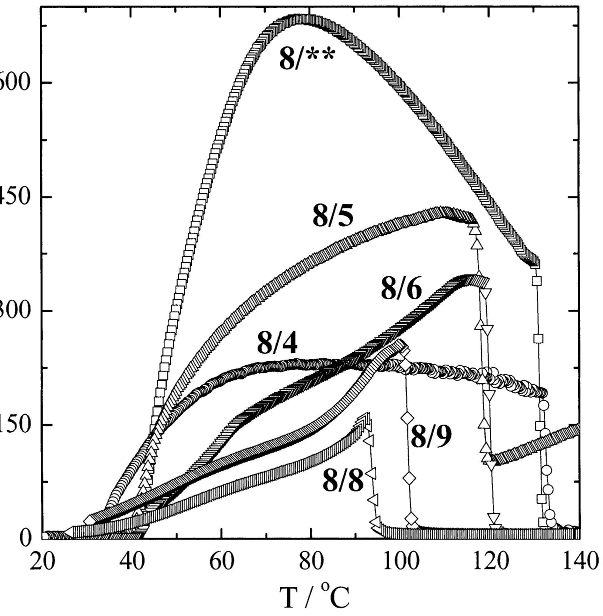

Figure 6. Temperature dependence of the real part of complex permittivity (ε′) for **K8/*n*** compounds measured on cooling at a frequency of 100 Hz.

4. Discussion and conclusions

Two new series of liquid crystals containing the keto group and two ester groups in the molecular core, and showing wide temperature range SmA and SmC* phases down to room temperature, were synthesized and studied. Increasing the non-chiral chain length has only a small influence on mesomorphic properties, while increasing the chiral chain length results in a broadening of the SmA phase and a shift of the ferroelectric SmC* phase to lower temperatures.

These compounds possess a very high spontaneous polarization, which reaches values up to 200 nC cm^{-2} for the homologues with two chiral centres. Similar compounds with the ether bridge instead of the keto group were studied by Taniguchi *et al.* and the maximum value of the spontaneous polarization was only about 50 nC cm^{-2} [5].

The helix pitch length remains essentially temperature-independent over the whole temperature range of the SmC* phase with the exception of the region immediately below the phase transition temperature. The helix pitch increases with the number of carbon atoms in the non-chiral chain and much more substantially with the number of carbon atoms in the chiral chain.

The compounds studied, with the keto group in the molecular core, would appear to be very useful as chiral dopants in mixtures for applications, due to the wide temperature range of the ferroelectric SmC* phase down to room temperature. A slight modification of the molecular structure to increase the transversal dipole moment may induce the antiferroelectric phase [6].

This work was supported by Grants No. 202/02/0840, No. 202/00/P044 and No. 106/00/0580 from the Grant Agency of the Czech Republic.

References

[1] Kumar, P. A., and Pisipati, V. G. K. M., 2001, *Mol. Cryst. Liq. Cryst.*, **365,** 1117.

[2] Yoschizawa, A., Nishiama, I., Fukumasa, M., Hirai, T., and Yamane, M., 1989, *Jpn. J. Appl. Phys.*, **28,** L1269.

[3] Bubnov, A., Hamplová, V., Kašpar, M., Glogarová, M., and Vaněk, P., 2000, *Ferroelectrics*, **243,** 27.

[4] Bubnov, A., Novotná, V., and Glogarová, M., 2002, presented at XV Czech–Polish Workshop on Structural and Ferroelectric Phase Transitions (Nechtiny Castle, Czech Republic), P-33; will be published elsewhere.

[5] Taniguchi, H., Ozaki, M., Yoshino, K., Satoh, K., and Yamasaki, N., 1988, *Ferroelectrics*, **77,** 137.

[6] Hamplová, V., Bubnov, A., Kašpar, M., Novotná, V., and Glogarová, M., 2002, presented at 19th International Liquid Crystal Conference (Edinburgh, Great Britain), P-252; will be published elsewhere.